ELSEVIER

Polymer 42 (2001) 2321–2330

polymer

www.elsevier.nl/locate/polymer

# Poly(styrene-*b*-isobutylene-*b*-styrene) block copolymers produced by living cationic polymerization. Part III. Dynamic mechanical and tensile properties of block copolymers and ionomers therefrom

R.F. Storey*, D.W. Baugh

*School of Polymers and High Performance Materials, The University of Southern Mississippi, Box 10076, Hattiesburg, MS 39406-0076, USA*

Received 12 January 2000; received in revised form 18 August 2000; accepted 18 August 2000

**Abstract**

Poly(styrene-*b*-isobutylene-*b*-styrene) (PS–PIB–PS) block copolymers prepared by living carbocationic polymerization and ionomers therefrom were analyzed using dynamic mechanical analysis (DMA) and tensile testing. The study encompassed five block copolymer samples, each with a PIB center block of approximately 52,000 g/mol, and PS weight fractions ranging from 0.127 to 0.337. Ionomers were prepared from two of these materials by lightly sulfonating the PS outer blocks. Sulfonation levels varied from 1.7 to 4.7 mol% and the sodium and potassium neutralized forms were compared to the parent block copolymers. DMA of the block copolymer films indicated the existence of a third phase attributed to PIB chains near the PS domain interface which experience reduced mobility due to their firm attachment to the hard PS domain. The relative amount of this phase decreased in samples with larger PS blocks, while the temperature of the associated transition increased. Tensile testing showed increased tensile strength but decreased elongation at break with larger PS blocks. DMA of the ionomers indicated improved dynamic modulus at temperatures above 90°C. Tensile testing of the ionomers indicated slight improvements in tensile strength with little loss in elongation at break. 

*Keywords*: Poly(styrene-*b*-isobutylene-*b*-styrene); Cationic polymerization; Dynamic mechanical analysis

## 1. Introduction

Thermoplastic elastomers (TPEs) display properties of conventional thermoset rubbers at normal use temperatures yet can be processed at elevated temperatures like conventional thermoplastics, e.g. by extrusion or injection molding. TPEs derive their unique properties from thermally reversible crosslinks, which are most often in the form of microphase-separated domains. This type of physical crosslinking has been produced in many types of polymeric systems including polyurethanes, polyesters, polyolefins, and block copolymers.

A common type of commercial TPE is based on A–B–A triblock copolymers, where the A blocks are polystyrene (PS) (minor component) and the B block is a diene-based rubber (major component). These materials are phase-separated due to the immiscibility of the component blocks; however macrophase separation is prevented by covalent bonds between dissimilar blocks. The morphology and mechanical properties of a given A–B–A block copolymer sample depend on several variables including the relative amounts of each component, block molecular weights, molecular weight distribution of each block, and sample preparation. The phase-separated domains are commonly in the form of spheres or cylinders of the minor component dispersed in a continuous matrix of the major component. The characteristic size of these domains is on the order of 10 nm, but is affected by block molecular weights.

The useful temperature range of A–B–A triblock-type TPEs is governed by the constituent polymers. Below the $T_g$ of the rubbery block the material is glassy while above the $T_g$ of the glassy phase, the physical crosslinks are easily deformed and significant creep or even flow can occur. It is possible to extend the upper use temperature significantly, and generally improve high temperature properties, by the introduction of thermally reversible, physical crosslinks into the PS domains, for example, by the introduction of ionic groups via sulfonation. This raises both the $T_g$ of the PS phase by about 2–4°C/mol% sulfonation [1,2] and may, depending on the level of sulfonation, create an additional phase (ionic clusters) with $T_g$s in excess of 300°C. Partial sulfonation of PS has also been shown to increase its thermal stability [3].

* Corresponding author. Tel.: +1-601-266-4868; fax: +1-601-266-5504.
*E-mail address:* robson.storey@usm.edu (R.F. Storey).

0032-3861/01/$ - see front matter 
PII: S0032-3861(00)00658-3

Table 1
Block copolymer compositions determined by NMR. PS block molecular weights were calculated based on NMR and GPC data as described in the text

| Sample | PIB $M_p$[a] | PS (vol%) by NMR | PS (wt%) by NMR | $M_n$ of PS blocks from NMR and GPC (g/mol) $\times 10^3$ |
|---|---|---|---|---|
| BCP05 | 49.9 | 11.3 | 12.7 | 3.6 |
| BCP04 | 51.9 | 17.2 | 19.2 | 6.2 |
| BCP01 | 53.0 | 23.1 | 25.5 | 9.1 |
| BCP03 | 53.8 | 30.6 | 33.5 | 13.6 |
| BCP02 | 51.7 | 30.8 | 33.7 | 13.1 |

[a] Peak molecular weight in GPC chromatogram.

Ionic modification at the low levels envisioned creates an ionomer, defined as a polymer containing up to about 15 mol% of ionic comonomers. Several morphological models for ionomers have been presented which explain various aspects of ionomer behavior such as their reduced melt flow, increased solvent resistance and enhanced toughness, especially at higher temperatures. One of the most recent, presented by Eisenberg et al. [4], describes the morphology of random ionomers as follows: ionic groups phase-separate from the non-polar polymer to form aggregates of 2–8 ion pairs, termed multiplets. These multiplets act as ionic crosslinks and are surrounded by matrix polymer chains, which experience reduced mobility due to their firm attachment at the ionic multiplet interface. The region surrounding the multiplets is termed the region of restricted mobility and extends a distance on the order of the persistence length of the polymer from the multiplet surface. As the ion content increases, more multiplets are formed and the regions of restricted mobility begin to overlap and eventually constitute a separate phase large enough to exhibit its own glass transition temperature. While multiplets raise the $T_g$ of the polymer matrix through the crosslinking effect, they are too small to exhibit their own $T_g$.

Weiss and coworkers [5–8] have produced lightly sulfonated poly(styrene-*b*-ethylene/1-butene-*b*-styrene) (SEBS) block copolymers. Small-angle X-ray scattering (SAXS) analysis of these block copolymer ionomers indicated two distinct levels of microphase separation, one characteristic of the glassy domains of the triblock copolymers previously discussed and one characteristic of ionic clusters dispersed in the PS domains. The authors envisioned a phase-separated morphology for the block copolymer ionomers consisting of ionic domains within the larger PS domains normally seen in this type of triblock copolymer. They also reported enhanced high temperature mechanical properties and development of a plateau in the modulus–temperature curve that persists well above the $T_g$ of PS [8].

Storey et al. [9,10] have produced block copolymer ionomers based on linear and three-arm star poly(styrene-*b*-isobutylene-*b*-styrene) (PS–PIB–PS) block copolymers which were synthesized by living cationic polymerization. They found that introduction of low levels (5–20 mol%) of sulfonate groups into the PS domains increased tensile modulus and tensile strength. They also observed an increase in thermal stability over the parent block copolymer, although the magnitude of the increase was not as large as that observed by Weiss et al. [8] for sulfonated SEBS block copolymers. It is significant that whereas the parent PS–PIB–PS block copolymers showed a very well-ordered phase-separated morphology by transmission electron microscopy (TEM), the derived ionomers displayed a virtually featureless field with no apparent contrast between phases. It was also noted that the ionomers are much more difficult to process by compression molding and are more sensitive to processing conditions than their parent block copolymers. Films were compression molded for 30 min at 120°C and 5000 psi for the parent block copolymers and for 12 h at 180°C and 15,000 psi for the ionomers. Longer heat treatments during compression molding had little effect on the block copolymer morphology and properties but had a significant effect on the mechanical properties of the ionomers.

In a series of papers we have reported detailed investigations of the composition [11] and morphology [12] of several PS–PIB–PS triblock copolymers, and ionomers derived therefrom, possessing similar PIB center blocks and PS outer blocks of varying sizes. This, the third paper of the series, focuses on the viscoelastic and mechanical properties of these materials using dynamic mechanical analysis (DMA) as a primary tool. These analyses were performed on films created using an optimized solvent casting technique, which afforded block copolymer ionomer films with well-developed microphase-separated morphologies very similar to those of the parent block copolymers. These morphologies were characterized in the second paper of this series [12] by SAXS and TEM.

## 2. Experimental

### 2.1. Materials

Linear PS-PIB-PS block copolymers were synthesized using a 1,3-di(2-chloro-2-propyl)-5-*tert*-butylbenzene/$TiCl_4$ initiating system employing pyridine as an externally added

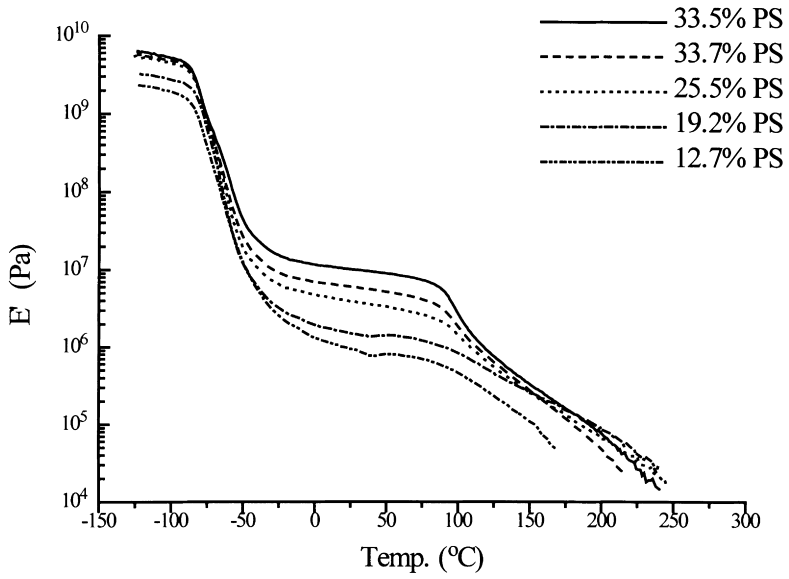


Fig. 1. Storage modulus ($E'$) vs. temperature curves for PS–PIB–PS block copolymers.

electron donor and di-*tert*-butyl pyridine (DTBP) as a proton trap in 60/40 (v/v) hexane/methyl chloride cosolvents at −80°C; details of the synthesis are reported elsewhere [11]. Compositions of the block copolymers, determined using proton NMR, are summarized in Table 1. PS block molecular weights were calculated from wt% PS determined by NMR and PIB inner block molecular weights (peak molecular weight, $M_p$) obtained by GPC.

Proton NMR was used to determine block copolymer composition in terms of weight fraction PS by comparing the integrated areas of the aliphatic and aromatic regions of the spectra [11]. Volume fraction PS was calculated for each sample using the densities 1.05 and 0.92 g/cm$^3$ for PS and PIB, respectively. Spectra were obtained using a 300 MHz Bruker ACE-300 NMR spectrometer. Samples were analyzed as 5% (w/v) solutions in $CDCl_3$, and reported against an internal reference (0 ppm) of tetramethylsilane (TMS).

High resolution GPC (HRGPC) was performed using a Shell Development Co. proprietary system, which employed a THF mobile phase at 50°C and dual refractive index (RI) and ultraviolet (UV) detectors. PIB molecular weights were referenced to PS standards.

### 2.2. Polymer sulfonation

The PS blocks of the triblock copolymer were lightly sulfonated using acetyl sulfate in refluxing methylene chloride. A portion of the sulfonated polymer solution (5 wt% in toluene with 1–2% (v/v) *n*-hexanol as polar cosolvent) was then titrated to a thymol blue endpoint using 0.05N ethanolic KOH or NaOH to determine the level of sulfonation. The remainder of the sample solution was then fully neutralized by slowly adding the appropriate amount of a methanolic KOH or NaOH solution to a refluxing solution of the sulfonated polymer. The resulting ionomer was recovered from solution by precipitation into methanol or ethanol. The precipitate was dried to constant weight in vacuum and later redissolved for film casting. The above procedure is discussed in detail in the second paper of this series [12].

Block copolymer films were cast into polytetrafluoroethylene (PTFE) lined pans from 5% (w/v) solutions in tetrachloroethylene (TCE) and dried at 50°C for seven days before being placed in a vacuum oven for further drying and annealing. Ionomer films were produced under identical conditions with the exception of the addition of 2–10% (v/v) *n*-hexanol to the solutions as a polar cosolvent. The film container was tightly covered with Al foil with several pinholes to slow solvent evaporation. Vacuum drying and annealing were carried out for 1 day at 60°C and then 3–5 days at 130–145°C.

DMA spectra were obtained using a Seiko Instruments model SSC/5200H dynamic mechanical spectrometer equipped with a DMS 210 tensile module. Rectangular samples possessing gage lengths of 20 mm and having cross-sectional areas of 8–13 mm$^2$ were utilized for tensile mode. Multiplexed (0.1, 1, 5, 10, and 20 Hz) spectra were obtained by sweeping temperature at a rate of 2°C/min from −120°C to ~325°C. Single frequency spectra were obtained at 1 Hz using a heating rate of 5°C/min. Curve resolution of tan $\delta$ data was performed using PeakFit software by Jandel Scientific. An exponential background and Gaussian peaks were used.

Tensile properties were measured using an MTS Model 810 Universal Test Machine equipped with a 100 lb load cell. Microdumbell samples with a gage length of 11.0 mm and width of 1.7 mm were cut from films 0.8–1.3 mm thick. The strain rate was 1.0 mm/s and 5–8 specimens of each sample were tested.

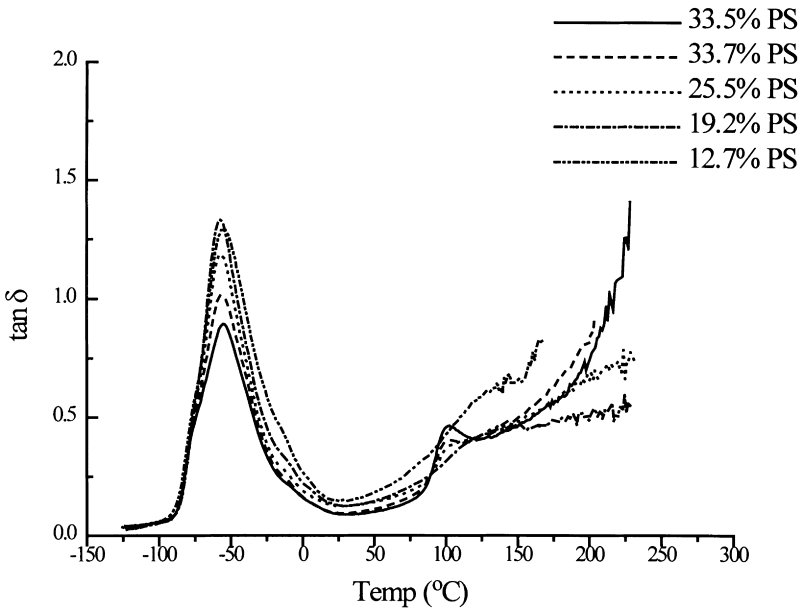


Fig. 2. Tan $\delta$ vs. temperature curves for PS–PIB–PS block copolymers.

## 3. Results and discussion

### 3.1. Sample preparation

Films of PS-PIB-PS block copolymers and ionomers were carefully cast from dilute solution with the objective of achieving equilibrium or near-equilibrium morphologies. Although it is considered best to choose a solvent whose solubility parameter falls midway between those of the two blocks, in the present case films were cast from TCE, which is slightly preferential for the PS blocks. The more neutral solvent, toluene, was considered, but was found to yield noticeably poorer films, which exhibited surface roughness including small pits and bubbles, and were cloudy. The higher boiling point of TCE (121°C) also allowed slower evaporation at elevated temperatures, which was found to be important when casting films of ionomers.

The ionomers also required addition of 2–10 vol% *n*-hexanol as polar cosolvent. The latter was chosen to match the evaporation rate of the primary solvent, preventing gel formation which occurs when the cosolvent evaporates first. This procedure produced films of nearly ideal or equilibrium morphology as evidenced by identical DMA results before and after annealing at 225°C for 30 min and slow cooling, over 2.5 h, to below 100°C. Films cast under less ideal conditions, i.e. with a deficiency of polar cosolvent or one that evaporates too quickly, exhibited dramatic differences in dynamic mechanical properties after one heating cycle in the DMA. This will be discussed in more detail in a subsequent section.

### 3.2. PS–PIB–PS dynamic mechanical analysis

The dynamic mechanical properties of the five PS-PIB-PS samples were typical of immiscible block copolymers. Figs. 1 and 2 show storage modulus ($E'$) vs. temperature and tan $\delta$ vs. temperature curves, respectively, of block copolymers containing 12.7–33.7 wt% PS. All films showed a drop in storage modulus at approximately −55°C, which corresponds to the $T_g$ of the PIB phase. A well-developed rubbery plateau was observed in the approximate temperature range −50–100°C, and the value of the rubbery modulus increased with increasing PS content. Samples with higher PS contents exhibited a second distinct transition

Table 2
PIB and PS $T_g$ and $T_g$ peak widths at half maximum obtained from tan $\delta$ vs. temperature curves acquired at 1 Hz with a 5°C/min heating rate

| Sample | PS (wt%) | PIB $T_g$ (°C) | PIB $T_g$ WHM[b] (°C) | PS $T_g$ (°C) | PS $T_g$ WHM[b] (°C) | PS $T_g$ Predicted (°C) |
|---|---|---|---|---|---|---|
| BCP05 | 12.7 | −56.2 | 35.2 | [a] | [a] | 76.4 |
| BCP04 | 19.2 | −57.8 | 29.6 | [a] | [a] | 86.3 |
| BCP01 | 25.5 | −57.5 | 32.0 | 106.7 | 29.8 | 90.7 |
| BCP03 | 33.5 | −57.1 | 37.1 | 103.0 | 25.9 | 93.8 |
| BCP02 | 33.7 | −57.4 | 35.0 | 102.0 | 23.9 | 93.5 |

[a] No PS $T_g$ was observable in tan $\delta$ vs. temperature curves for these samples; however the PS $T_g$ is clearly shifting to lower temperatures with decreasing wt% PS, as seen in the $E'$ vs. temperature curves.
[b] Peak width at half maximum.

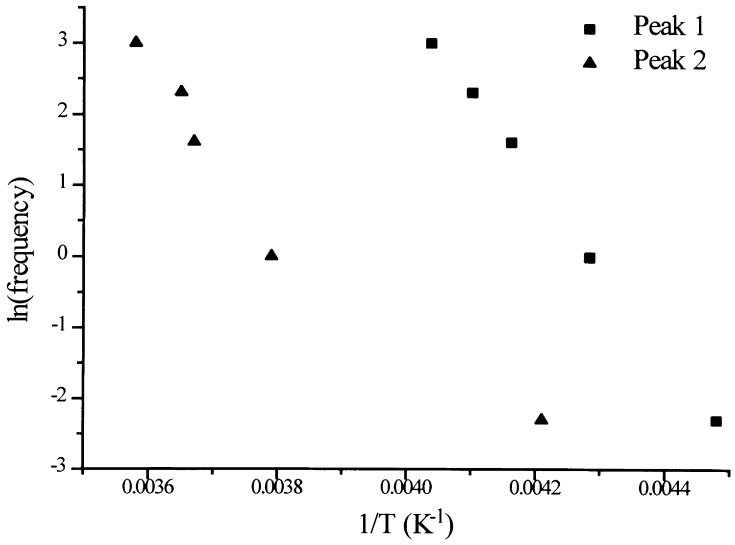


Fig. 3. Arrhenius plot for two tan $\delta$ component peaks of the PIB $T_g$ in PS-PIB-PS sample containing 33.5 wt% PS.

near 100°C, which corresponds to the PS $T_g$. This transition became broader and shifted to lower temperatures for the samples containing 19.2 and 12.7% PS. One might have suspected that the PS blocks in these samples are too small to phase separate into discrete domains; however SAXS studies from the previous paper showed that the sample containing 19.2 wt% PS does form cylindrical PS domains with sharp phase boundaries [12]. Furthermore, large amounts of phase mixing would have resulted in broadening and shifting of the PIB $T_g$, but there was no indication of this.

Table 2 lists the $T_g$ and width at half maximum (WHM) of the $T_g$ peak, obtained from tan $\delta$ vs. temperature curves for the PIB and PS phases for each sample. Clearly the $T_g$ and the width of the transition for the PIB phase in each sample remained approximately constant at −57 and 34°C, respectively. Although the PS $T_g$ cannot be accurately measured by DMA for the 19.2 and 12.7% PS samples, it was apparent from Fig. 1 that the transitions shifted to lower temperatures and broadened with decreasing PS content. This observed decline in PS $T_g$ with lower PS block length is most readily explained by the effect of molecular weight on $T_g$, as predicted by the Fox–Flory equation, $T_g = T_g^\infty - (c/M_n)$ [13]. This relationship was derived from free-volume theory to account for the fact that free-volume around chain ends is greater than around chain middles due to imperfect packing at the chain ends. For linear homo-PS, $c = 1.7 \times 10^5$ g/mol and $T_g^\infty \approx 100$°C [14]. The Fox–Flory equation was not expected to apply directly to the present system because for a PS block of a given size, only one PS chain end exists while the other end is covalently bonded to a PIB chain. For purposes of calculating a predicted PS $T_g$ in the present context, the block molecular weights were doubled, resulting in the proper number of chain ends for a given PS block molecular weight. The predicted $T_g$s thus obtained are listed in the last column in Table 2. Although lower than the experimental values, the calculated $T_g$s show that the PS $T_g$ should be relatively constant for PS blocks above about 9000 g/mol, but then should fall rapidly as the block length decreases. This is precisely the trend qualitatively observed in Fig. 1.

The loss tangent behavior of high molecular weight homo-PIB is known to exhibit a unique high-frequency (lower temperature) shoulder. In 1995 Plazek et al. [15] investigated the difference in temperature dependence of the two transitions with the goal of clarifying the origin of the unique two-peak structure. Close examination of the PIB glass transition region in the tan $\delta$ curves of Fig. 2 revealed what appear to be three overlapping peaks, with the main peak centered at −55°C. It was apparent that the main transition and the low temperature shoulder arose from the PIB glass transition and are the two components discussed by

Table 3
Results of Arrhenius plots of deconvoluted PIB $T_g$ tan $\delta$ peaks from multifrequency DMA

| Sample | PS (wt%) | Peak 1 $E_{act}$ (kJ/mol) | Correlation coefficient | Peak 2 $E_{act}$ (kJ/mol) | Correlation coefficient |
|---|---|---|---|---|---|
| BCP05 | 12.7 | 118.9 | −0.9976 | 80.1 | −0.9953 |
| BCP04 | 19.2 | 120.5 | −0.9984 | 78.9 | −0.9856 |
| BCP01 | 25.5 | 111.6 | −0.9952 | 93.8 | −0.9921 |
| BCP03 | 33.5 | 101.0 | −0.9996 | 67.9 | −0.9677 |
| BCP02 | 33.7 | 100.1 | −0.9990 | 69.6 | −0.9731 |

Table 4
PIB $T_g$ component peak data derived from deconvolution of 1 Hz data in multifrequency DMA at 2°C/min heating rate. Peak position, width at half maximum, and percent area are shown

| Sample | PS (wt%) | Peak 1 Temp. (°C) | Peak 1 WHM[a] (°C) | Peak 1 (%) area | Peak 2 Temp. (°C) | Peak 2 WHM[a] (°C) | Peak 2 (%) area |
|---|---|---|---|---|---|---|---|
| BCP05 | 12.7 | −43.5 | 30.1 | 67.0 | −25.3 | 41.6 | 33.0 |
| BCP04 | 19.2 | −41.8 | 30.6 | 67.3 | −23.6 | 47.3 | 32.7 |
| BCP01 | 25.5 | −41.1 | 34.3 | 76.8 | −17.0 | 47.7 | 23.2 |
| BCP03 | 33.5 | −39.7 | 37.5 | 85.8 | −9.2 | 50.3 | 14.2 |
| BCP02 | 33.7 | −40.2 | 36.7 | 85.5 | −12.7 | 48.6 | 14.5 |

[a] Peak width at half maximum.

Plazek et al. The more prominent high temperature shoulder appeared to be unique to the block copolymers and also varied with PS content. To further investigate the nature and origin of this high temperature peak, we performed multifrequency DMA on the series of block copolymers. Curve resolution of the tan $\delta$ plots then allowed apparent activation energies for each component peak to be calculated from Arrhenius plots of ln(frequency) vs. $1/T$. For the purposes of this analysis, the two components of the PIB glass transition were treated as one peak while the high temperature shoulder was treated as a second peak. This was necessary due in part to the lower data density of the multifrequency DMA data which made the lowest temperature peak unresolvable. Fig. 3 shows typical Arrhenius plots for the two component peaks, in this case for the sample containing 33.5 wt% PS. Here, as in all cases, the lower temperature peak yielded a very linear Arrhenius plot while the high temperature peak yielded sigmoidal curves. Table 3 lists apparent activation energies and correlation coefficients of the linear fits derived from Arrhenius plots for the five block copolymer samples. Apparent activation energies for the low temperature peak (Peak 1) are relatively constant and as shown in Fig. 3 are the result of very good linear fits to the data. Apparent activation energies for Peak 2 are consistently lower by 20–30 kJ/mol, but are derived from poorer linear fits and therefore vary more from sample to sample. The differences in apparent activation energies and in the shapes of Arrhenius plots for the two peaks suggests that the molecular motions associated with the two peaks are quite different.

We next investigated the relative positions, widths, and areas of the two component peaks with the goal of gaining further insight into their origin. Table 4 shows the results of curve resolution of the two component peaks discussed above. The 1 Hz data from multifrequency DMA performed at a heating rate of 2°C/min were used for Table 4. In all samples, the low temperature peak remained relatively unchanged in position and width while the high temperature peak shifted dramatically in temperature and somewhat in width with increasing PS content. A dramatic change in the relative areas of the two component peaks was also seen. For the lowest PS content, the ratio of the low temperature peak area to that of the high temperature peak was 2:1 while for the highest PS content it was 5.9:1. These changes in the temperatures and relative areas of the two component peaks suggest that the high temperature peak is the result of PIB chain segments near the interface which experience reduced mobility due to their attachment to the hard PS domain. This is analogous to the region of restricted mobility surrounding ionic multiplets in ionomers as postulated by Eisenberg et al. [4]. These authors also predicted a very similar phenomenon for A-B-A block copolymers. The lower temperature

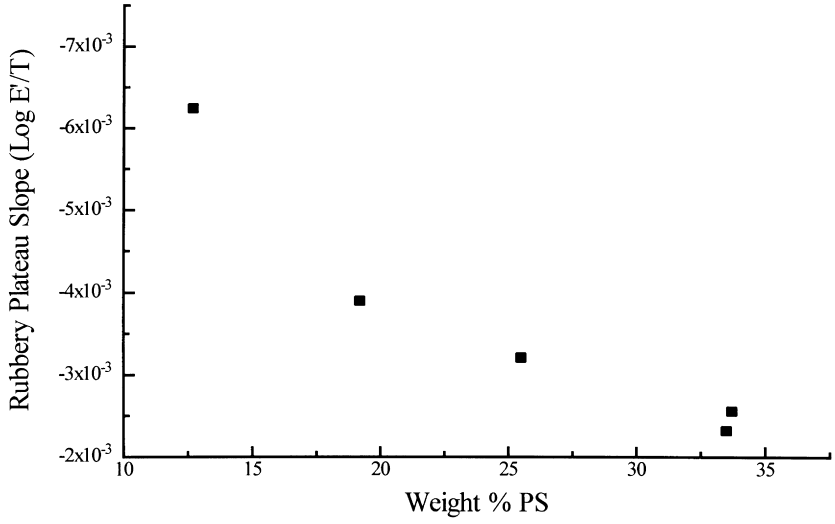


Fig. 4. Plot of rubbery plateau slope vs. wt% PS for five PS-PIB-PS block copolymers.

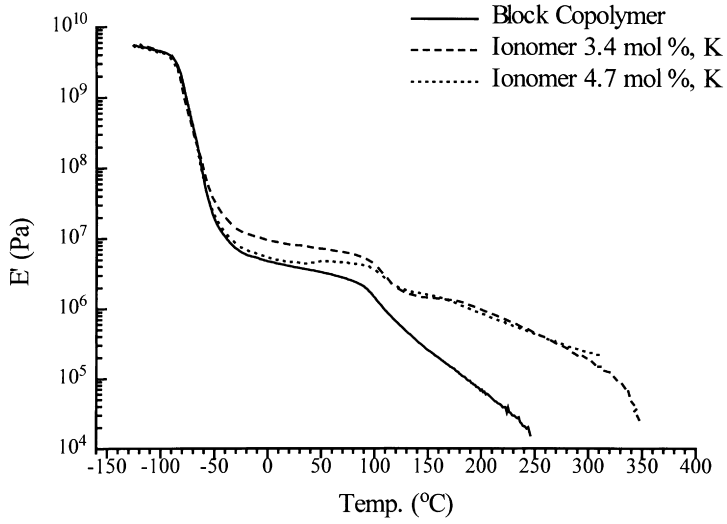


Fig. 5. Storage modulus ($E'$) vs. temperature curves for 25.5 wt% PS block copolymer and block ionomers therefrom.

peak originating from the pure PIB phase remained relatively unchanged in all five samples, while the high temperature peak, originating from PIB near the interface, occurred at higher temperatures with increasing PS block size due to the higher $T_g$ of the associated PS block. The lower apparent activation energy of the high temperature peak is also consistent with the lower apparent activation energies of the cluster-phase glass transitions in ionomers [16–18].

Another aspect of the $E'$ vs. temperature curve which relates to the degree of phase mixing in an immiscible block copolymer system is the slope in the modulus plateau at temperatures between the two glass transitions, i.e. the slope of the rubbery plateau. Immiscible block copolymers usually exhibit modulus–temperature behavior similar to that of polymer blends in which each component retains its identity and exhibits its own $T_g$. The resulting modulus–temperature curves display two distinct transitions, each at or near the $T_g$ of the respective homopolymer, with a constant modulus plateau between the two glass transitions. The relative amount of each component determines the position, or height, of the plateau while the flatness of the plateau is dependent on the degree of phase separation; the more complete the phase separation, the more temperature insensitive the modulus becomes [19]. Therefore, the storage modulus vs. temperature curve provides an indication of the quality of phase separation; phase mixing results in broadening and/or temperature shifts in the observed glass transition temperatures and in larger negative slopes in the modulus plateau at temperatures between the two glass transitions. Fig. 4 is a plot of the slope of (log($E'$) vs. temperature) vs. wt% PS for the five samples studied. The data clearly show that the absolute value of the rubbery plateau slope consistently increases with lower PS contents

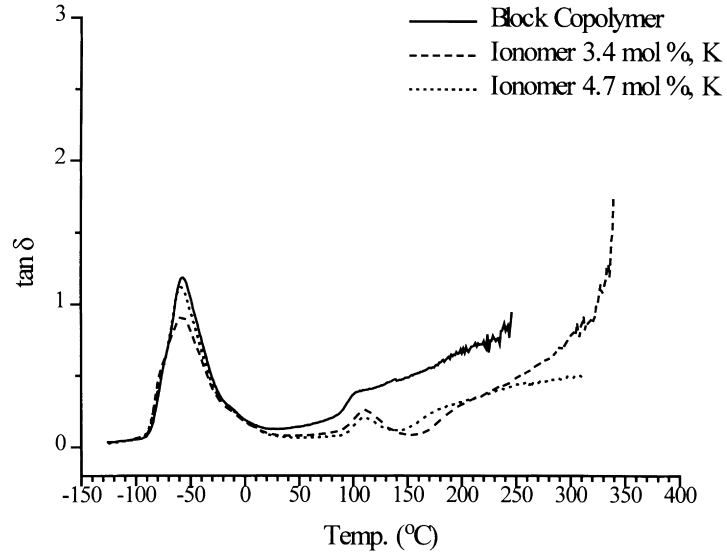


Fig. 6. Tan $\delta$ vs. temperature curves for 25.5 wt% PS block copolymer and block ionomers therefrom.

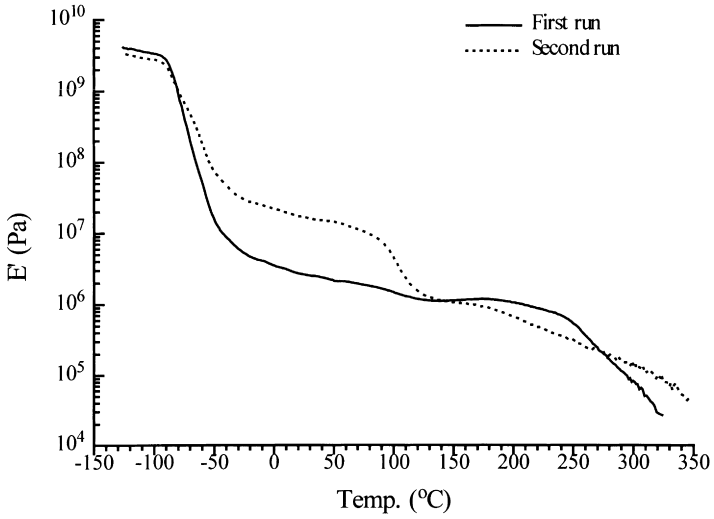


Fig. 7. Storage modulus ($E'$) vs. temperature curves for PS–PIB–PS ionomer containing 1.7 mol% sodium sulfonate groups showing the effect of non-equilibrium morphologies on dynamic mechanical properties.

or smaller PS blocks. This result indicates that increased phase mixing occurs with smaller PS blocks. Porod analysis of SAXS data in the second paper of this series [12] indicated that all of the samples were characterized by sharp phase boundaries; therefore these results indicate that isolated phase mixing occurs within the domains.

### *3.3. PS–PIB–PS ionomer dynamic mechanical analysis*

Ionomers produced by sulfonating 3.4 and 4.7 mol% of the styrene units in the PS blocks of BCP01 (25.5 wt% PS) were analyzed by DMA for comparison with the parent block copolymer. Figs. 5 and 6 show $E'$ vs. temperature and tan $\delta$ vs. temperature, respectively, for the parent block copolymer and the potassium neutralized form of the two ionomers. Below approximately 90°C, the parent block copolymer and the ionomer with lower ion content (3.4 mol%) displayed virtually identical behavior except that the rubbery plateau modulus was somewhat higher for the ionomer. In contrast, the ionomer with 4.7 mol% ion groups displayed an initial plateau modulus approximately identical to the parent, but then displayed a modulus increase that began at approximately 40°C. However, the modulus never reached the value of the 3.4 mol% sample, and the PS phase glass transition is less defined. The modulus increase beginning at 40°C is apparently due to reorganization, driven by the thermal and mechanical energy imparted by the experiment, of non-equilibrium structures that remained in the sample with higher ion content. Support for this interpretation is given in Fig. 7, which shows storage

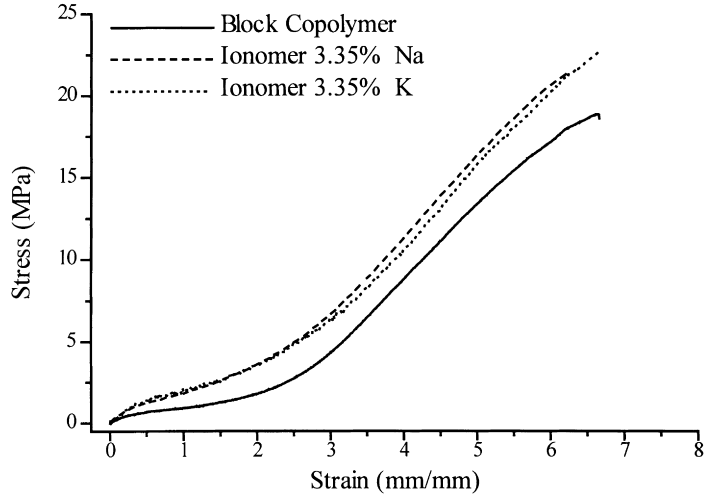


Fig. 8. Typical stress–strain curves for PS–PIB–PS block copolymers (25.5 wt% PS sample shown) and comparison of Na and K neutralized ionomers therefrom.

Table 5
Results of tensile testing of PS–PIB–PS block copolymers and block ionomers

| | BCP05 12.7% PS | BCP04 19.2% PS | BCP01 25.5% PS | BCP02 33.7% PS | BCP03 33.5% PS | BCP01 ionomer 3.35% Na | BCP01 ionomer 3.35% K |
|---|---|---|---|---|---|---|---|
| Tensile strength (MPa) | 10.12 | 17.12 | 18.97 | 20.32 | 21.31 | 22.81 | 23.18 |
| Std. deviation (%) | 9.23 | 1.30 | 3.75 | 4.25 | 3.21 | 3.80 | 6.76 |
| Strain at break (%) | 868.3 | 828.7 | 680.1 | 633.7 | 514.1 | 627.3 | 664.7 |
| Std. deviation (%) | 4.20 | 0.84 | 3.18 | 2.12 | 4.14 | 3.42 | 8.52 |

modulus vs. temperature curves, obtained in two consecutive runs, for a PS–PIB–PS ionomer with 1.7 mol% Na sulfonate groups. This sample was clearly in a non-equilibrium state as evidenced by the profound difference between the first and second DMA runs. The important point is that the plateau modulus is initially lower, and the PS phase glass transition is poorly defined. Once the sample has been annealed during the first run, the second run reveals a significantly higher plateau modulus and well-defined PS phase glass transition, similar to the 3.4 mol% ionomer in Fig. 5. Figs. 5 and 6 further reveal that, upon reaching the $T_g$ of the PS phase, the response of the two ionomers was approximately the same. Dramatic differences between parent and ionomer were seen above the $T_g$ of PS. The ionomers exhibited a second small plateau modulus followed by a gradual decrease in modulus from about 180 to over 300°C. The magnitude of the drop in storage modulus was slightly larger for the ionomer with the lower level of sulfonation. This has been noted in several similar ionomer samples we have produced, and this transition seems to disappear for Na and K ionomers with sulfonation levels above approximately 10 mol%, resulting in a relatively constant modulus plateau from −30 to over 300°C [10,20]. This ion content is near that at which the ionic cluster phase becomes dominant in conventional PS ionomers [18]. For samples with less than $\approx 10$ mol% sulfonation, the absence of changes in this transition on subsequent DMA runs on the same sample is diagnostic of well-developed, near-equilibrium morphologies. Both ionomers showed a considerably lower loss tangent compared to the parent, indicating higher resiliency imparted by the presence of the strongly interacting ionic groups within the PS dispersed phase. In both the $E'$ and tan $\delta$ spectra, the $T_g$ of the PS phase was clearly visible and higher in the ionomers than in the parent block copolymers, as is typical of ionomers.

### *3.4. PS–PIB–PS block copolymer and block ionomer tensile properties*

Fig. 8 shows the stress–strain curves for the PS–PIB–PS block copolymer containing 25.5 wt% PS and the sodium and potassium neutralized ionomers therefrom. These curves are typical of the materials in the present study. The results for all five samples and the two ionomers are listed in Table 5. As is typical for styrenic A–B–A block copolymer TPEs, the peak stress at break decreased with decreasing PS content while the elongation at break increased. In ionomers with relatively low ion contents, as shown in Figs. 5 and 7, the dynamic mechanical and tensile properties are virtually unchanged, compared to the block copolymer precursor, at temperatures below 90°C, while dynamic modulus is significantly enhanced at temperatures above 100°C. This property could be quite useful when one desires a material with enhanced high temperature properties without changes in low temperature properties.

## 4. Conclusions

The PS–PIB–PS block copolymers in this study behaved largely as expected for this class of A–B–A block copolymers, exhibiting two distinct transitions in $E'$ vs. temperature plots. The existence of a third phase, consisting of PIB chain segments near the hard PS domain interface which experience reduced mobility due to their attachment at the interface, was evident upon close scrutiny of tan $\delta$ peaks. Apparent activation energies for this transition were lower than for the main PIB phase, just as is seen in cluster-phase glass transitions in ionomers. The temperature of this transition also increased with increasing PS block size, paralleling the increase in $T_g$ of the larger PS blocks. Evidence of increasing amounts of phase mixing with decreasing PS block size was obtained by examining the rubbery plateau slope as a function of PS content.

The PS–PIB–PS ionomers exhibited improved dynamic storage modulus above 100°C and slightly increased tensile strength while maintaining properties nearly identical to their block copolymer precursor at temperatures below 100°C. Dramatic improvements in sample preparation resulted in near-equilibrium morphologies, which provided very reproducible and more meaningful dynamic mechanical and tensile data for the ionomers than has been shown before.

## References

[1] Wallace RA. J Polym Sci, Part A-2 1971;9:1325.
[2] Mattera Jr. VD, Risen Jr. WM. J Polym Sci, Polym Phys Ed 1986;24:753.
[3] Lantman CW, MacKnight WJ, Lundberg RD. Proc North Atlantic Therm Anal Soc, San Francisco, CA 1985:236.
[4] Eisenberg A, Hird B, Moore RB. Macromolecules 1990;23:4098.
[5] Weiss RA, Sen A, Pottick LA, Willis CL. Polymer 1991;32(10):1867.
[6] Weiss RA, Sen A, Pottick LA, Willis CL. Polymer 1991;32(15):2785.
[7] Weiss RA, Sen A, Willis CL, Pottick LA. Polym Commun 1990;31:221.
[8] Weiss RA, Steckle WP, Lu X. Polym Mater Sci Engng 1991;65:240.
[9] Storey RF, Chisholm BJ, Lee Y. ACS Div Polym Chem, Polym Prepr 1992;33:184.
[10] Storey RF, Chisholm BJ, Lee Y. Polym Engng Sci 1997;37(1):73.
[11] Storey RF, Baugh DW, Choate KR. Polymer 1999;40:3083.
[12] Storey RF, Baugh DW. Polymer 2000;41(9):3205.
[13] Fox TG, Flory PJ. J Appl Phys 1950;21:581.
[14] Aklonis JJ, MacKnight WJ. Introduction to polymer viscoelasticity. New York: Wiley, 1983 (chap. 4).
[15] Plazek DJ, Chay I-C, Ngai KL, Roland CM. Macromolecules 1995;28:6432.
[16] Kim J-S, Eisenberg A. J Polym Sci, Part B: Polym Phys 1995;33:197.
[17] Kim J-S, Roberts SB, Eisenberg A, Moore RB. Macromolecules 1993;26:5256.
[18] Hird B, Eisenberg A. J Polym Sci, Part B: Polym Phys 1990;28:1665.
[19] Noshay A, McGrath JE. Block copolymers: overview and critical survey. New York: Academic Press, 1977 (chap. 4).
[20] Storey RF, Baugh DW. Unpublished results.